

Density of Superheated and Undercooled Liquid Alumina by a Contactless Method¹

B. Glorieux,² F. Millot,^{2,3} J.-C. Rifflet,² and J.-P. Coutures²

The density of liquid alumina drops maintained in levitation with an aerodynamic device and heated with CO₂ lasers is determined by analysis of high-speed video digital images between 2000 and 3100 K in various gases. It is shown that consistent results can be achieved for the lighter drops ($m < 100$ mg) which do not depend on the nature of the gas. Experiments performed with lasers impinging the drop surface or during free cooling of the preheated drop gave similar results. The density is represented by the following expression: $d = (2.79 \pm 0.01)(1 - \alpha(T - 2500)) \text{ g} \cdot \text{cm}^{-3}$, where $\alpha = (4.22 \pm 0.14) \times 10^{-5} \text{ K}^{-1}$.

KEY WORDS: contactless techniques; density; high-speed digital video; high temperatures; laser heating; liquid alumina.

1. INTRODUCTION

Liquid alumina properties are difficult to assess because of the high temperatures involved and because of the chemical pollution, which is particularly difficult to avoid unless contactless techniques are used. Some density measurements have been reported on liquid alumina [1–10]. Most of them [1–8] were obtained under conditions that cannot preclude chemical pollution of the liquid. In recent years it has been proposed by Grannier and Heutault [9] and later by Coutures et al. [10] to determine the density of a liquid of known weight from an image analysis of an approximately spherical aerodynamically levitated droplet. The results obtained so far are moderately accurate. It is the object of this work to assess the

¹ Paper presented at the Fifth International Workshop on Subsecond Thermophysics, June 16–19, 1998, Aix-en-Provence, France.

² Centre de Recherches sur les Matériaux à Hautes Températures (CRMHT), CNRS, 1D avenue de la Recherche Scientifique, 45071 Orléans, France.

³ To whom correspondence should be addressed.

methodology of contactless density measurement and to use new facilities offered by a digital high-speed videocamera to obtain reliable density data for high-temperature liquids. The emphasis is on liquid alumina density, which is important in various fields.

- Propergol combustion produces high-temperature liquid alumina in rockets. Therefore, liquid alumina properties are important for the combustion model of these engines.
- Liquid alumina is a constituent of many glasses. The prediction of their density from thermodynamics of mixtures requires accurate data on the density of liquid alumina [11].

2. EXPERIMENTAL PROCEDURE

Two experimental setups were used in this study, which we describe below.

2.1. Firsts Setup

An alumina droplet, having a diameter of a few millimeters, is levitated with a flow of gas passing through a convergent–divergent nozzle (see Ref. 10). It is heated from the top with a 600-W CO₂ laser ($\lambda = 10.6 \mu\text{m}$), and the temperature of the upper part of the drop is recorded with a pyrometer operating at $5.5 \mu\text{m}$ and calibrated with the melting temperature of alumina ($2327 \pm 8 \text{ K}$) [10]. The temperature of the liquid drop is not uniform as a consequence of the directional nature of the laser heating. However, if one cuts off the laser and then allows the drop to cool freely, the temperature of the droplet becomes spatially more uniform after $\tau \approx 100 \text{ ms}$. If we consider the latter value, we can deduce, for a 3-mm drop, an approximate temperature difference of 30 K between the surface and the center during the cooling of the liquid. It is then possible to do measurements on a homogeneous liquid during the 2 s of cooling before the crystallization of the undercooled liquid.

2.2. Second Setup

An alumina droplet is levitated in a specially designed biconic nozzle. The main characteristic of the nozzle is that it performs a double function. The upper part is for levitation, and the lower one is an optical concentrator for a CO₂ laser beam having an 8-mm diameter. The drop is then heated with two lasers, one impinging on the top and the other on the bottom. The power of the lasers (120 W each) is adjusted in order to have the

same temperature measured with two pyrometers ($\lambda = 0.85 \mu\text{m}$) pointing, respectively, to the top and to the bottom of the droplet. Examination of the brightness with a camera indicates that the temperature variations of the droplet surface may be as large as 100 K. This device allows measurements on the nearly homogeneous drop with laser heating at some temperature or, alternatively, during the free cooling as before.

2.3. Camera Device

The top of the alumina droplet is observed with a digital high-speed camera (Kodak Ektapro, 1000HRC) having a 512×384 -pixel image area. There are 256 gray levels for every pixel. The speed of recording is 1000 frames per s, with an exposure time varying from $50 \mu\text{s}$ to 1 ms. Frames are recorded on a magneto-optical disk that can be easily used in a computer. The temperatures measured with the pyrometer are inserted in every frame with a special interface system.

We proceeded to optical focusing of the drop just before cutoff of the laser in order to achieve the optimum quality of the image. We also varied the light collected by the camera during the cooling with a manual adjustment of a polarizing filter in order to get the maximum contrast between the droplet and the background without overexposure.

For every frame, the apparent temperature T is deduced from the signal V of the pyrometer:

$$T = C_2 / (\lambda \cdot \ln((k + V)/V)) \quad (1)$$

where C_2 is Planck's second radiation constant, which is equal to $1.4388 \times 10^{-2} \text{ m} \cdot \text{K}$, λ is the pyrometer wavelength, and k is a parameter calculated at $2327 \pm 8 \text{ K}$ for the solidification plateau observed after the recalescence due to the crystallization of undercooled liquid Al_2O_3 [10].

We note that the cooling law observed with the $5.5\text{-}\mu\text{m}$ pyrometer follows a $1/T^3$ straight-line behavior versus time, which is characteristic of purely radiative cooling. Adjusted values of the temperature were deduced from that curve.

2.4. Density Measurements and Data Processing

The density is measured as the ratio of the weight to the volume under the assumption that the levitated droplet is spherical. Its volume is then deduced from the measurement of the surface and the weight obtained after the cooling of the drop. Weight losses during the experiment are small

(<0.5%), and they are related mainly to evaporation during stabilization of the droplet and focusing.

In order to make good surface measurements from the images obtained by the camera, it is first necessary to be able to determine the number of pixels for this surface area. Powerful image processing software (Visilog5) can be used to determine the edge length and to calculate the area.

In order to obtain the best results in a reasonable time, the following procedure was used.

- Maximum brightness values are normalized to 255 for every image.
- A multidirectional gradient technique is used to produce a picture of the gradient of the intensity of the image.
- A threshold function converts this frame to a binary image because the edge of the drop corresponds to the maxima of the gradient intensity.
- We choose this threshold value to find a binary image that corresponds to a closed ring.

This selection method is fast (6 s for every frame), but it overestimates the area because, in some parts of the image of the drop, the threshold value is not just slightly above the maximum of the intensity. To calculate the area overestimation, we used a watershed function to determine the exact maximum intensity line. But a frame-by-frame treatment is needed because the watershed function selects every pixel which has a neighbor of lower intensity, and too many pixels would be selected. Many low-pass filters are used to avoid noise from a derivative frame, and therefore, the processing time is very long. Then we calculate the overestimation for 5% of the frames. The overestimation is about 1500 pixels for an area of 50,000 pixels. This mean value is systematically subtracted from the area value obtained with the threshold technique.

The calibration to convert the area from pixels to square centimeters is done with a transparent grid illuminated from the back side substituted in place of the levitation system. The reticle of known size allows edge measurements to better than 1 pixel. This calibration was performed only with the first setup. The volume V is finally determined under the provisional assumption of a spherical shape:

$$V = 0.752S^{3/2}$$

where S is the area of the droplet (cm^2).

The accuracy of the density measurement described previously is dependent on the sphericity of the levitated droplet. The observation with the camera from the top does not allow any conclusion about this concern. It is then necessary to vary parameters which could influence the sphericity in order to determine the reliability of this preliminary hypothesis. These parameters are the weight of the drop and, also, the nature of the gas and the temperature.

3. RESULTS AND DISCUSSION

A typical result obtained in oxygen during radiative cooling of a 14-mg droplet is shown in Fig. 1. It is worth noting that fluctuations of the area are visible with a characteristic frequency of a few hertz.

In order to reduce this fluctuation, we accumulated various sequences obtained under the same conditions. The averaging of the area is also shown in Fig. 1. It is clear that we reduce considerably the uncertainties in the part that we expect for random variation (from 3.5 to 1.4%) when we use this averaging procedure.

The view from the top of the drop as seen by the camera is an almost-perfect disk, with differences between orthogonal radii of less than 0.6%. However, we have no idea of the side shape, although we can easily imagine that big droplets are more sensitive to deformation than smaller

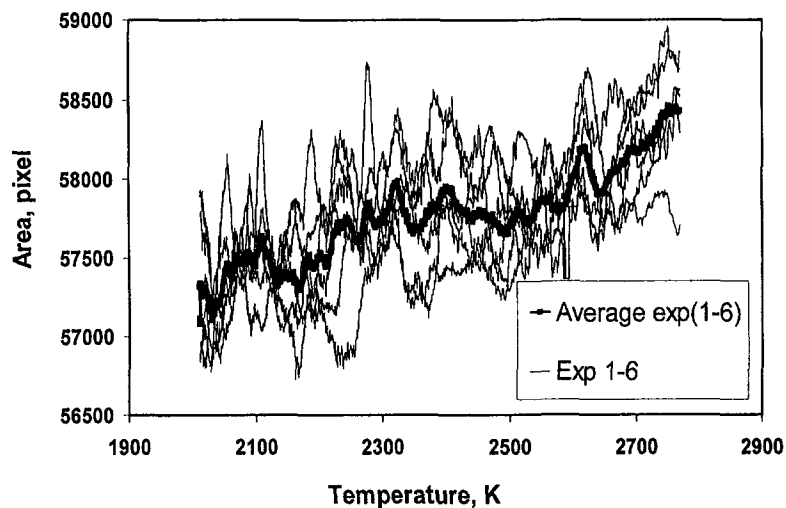


Fig. 1. Average of six area measurements of a 14-mg alumina droplet during free cooling under oxygen.

ones. Different-weight droplets, ranging from 14 to 150 mg were then studied in O_2 in order to observe their possible deviation from sphericity. Results based on the assumption of sphericity appear in Fig. 2 and show that, for droplets weighing less than 78 mg, the observed density is the same, apparently verifying the spherical assumption. However, the 150-mg droplet density is smaller, indicating that the droplet is slightly flattened.

Similar experiments were performed in an argon atmosphere with droplets weighing 38 and 78 mg. These experiments are not as easy in argon as in oxygen. It is difficult to melt the droplet completely and to obtain a stable levitation. The fluctuations of the surface area are significant, and nine experiments are needed to reduce the fluctuations to less than 1.5%. The results in Fig. 3 show a behavior different from that observed under oxygen, principally during the first moments of free cooling, which correspond to a transitory homogenization of the temperature of the droplet. During that time, the apparent density increases with temperature. It appears probable that the spherical assumption is not correct under argon when the temperature of the drop is already nonuniform. However, the fact that we obtain very comparable results in argon and oxygen on homogeneous drops of different weights indicates that the spherical assumption can be used.

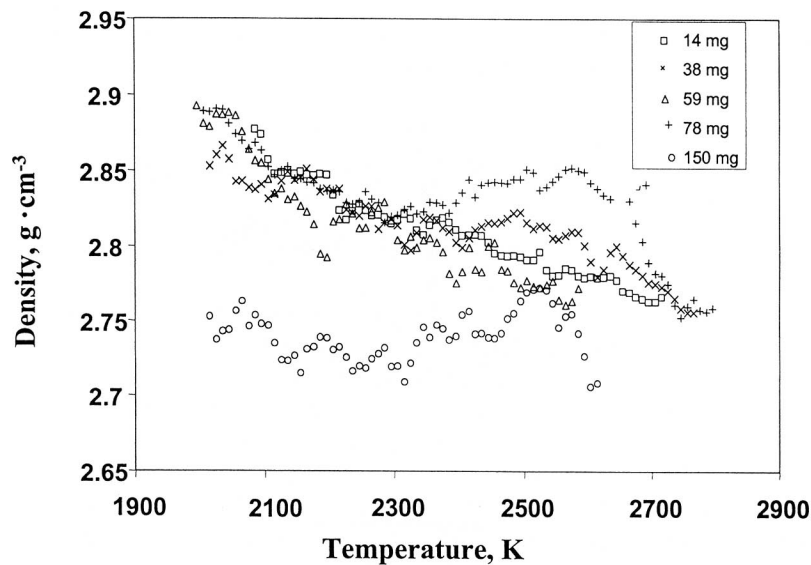


Fig. 2. Density of liquid alumina in oxygen for different droplets.

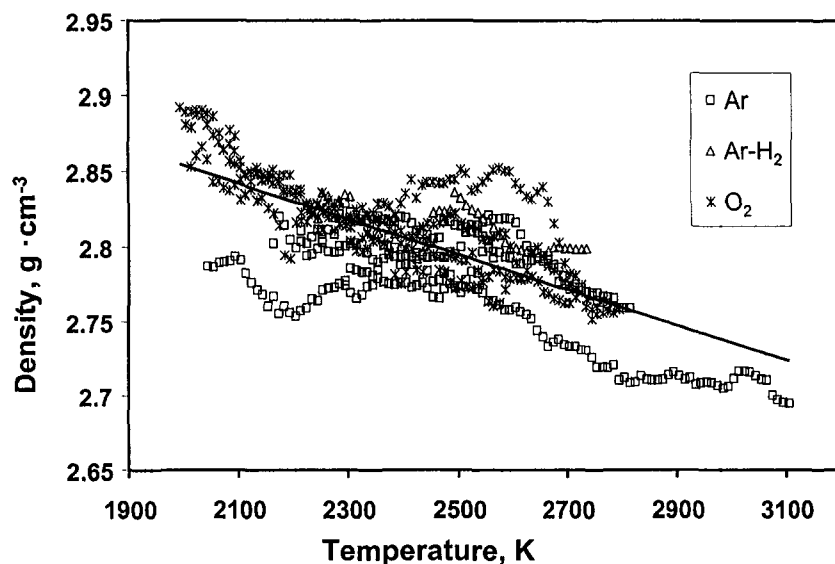


Fig. 3. Density of liquid alumina in various gases.

Noxal gas, 95% Ar–5% H₂, was also used to levitate liquid alumina. We observed a similar although magnified, behavior to that for argon gas: difficulties in melting and in levitating and anomalous behavior at the very beginning of the free cooling. The homogeneous liquid shows a density quite similar to that in the other gases.

All the results obtained in these various gases and corresponding to free cooling experiments from different initial temperatures are shown in Fig. 3. For the 600 averaged density values, a linear curve is a reasonable representation:

$$d = (2.79 \pm 0.01)(1 - \alpha(T - 2500)) \text{ g} \cdot \text{cm}^{-3}$$

where $\alpha = (4.22 \pm 0.14) \times 10^{-5} \text{ K}^{-1}$, with T ranging from 2000 to 3100 K. If we combine the various sources of errors (weight, 0.05%, droplet area in pixels, 2.3%; error introduced by the reticle area, 0.1%; calibration error with the reticle, 1%), we estimate a total uncertainty for a single density measurement of better than 5%, of which we would estimate a possible systematic error of 1.5%.

These results obtained with the free cooling technique are to some extent quite puzzling since we were able to obtain reproducible results when we used accumulated data in order to reduce the low-frequency changes in the area that we observed during every cooling sequence.

However, it is difficult to assess the origin of the low-frequency fluctuation, which is seen from the top as a respiration phenomenon of an almost-perfect circle. These observations could be, for example, the result of a rocking phenomenon during the cooling of the drop and, then, induced undesired systematic errors, mainly of the thermal expansivity term α .

We then performed experiments with the second setup in pure oxygen at a fixed temperature, and we obtained the density mean area of 200 successive images recorded under conditions of thermodynamical equilibrium with the gas. We used a 52-mg droplet, and two sets of experiments, 1 and 2, were performed under different optical settings. There was no calibration of the surface of a pixel, and the density data were arbitrarily adjusted to a reasonable value for every set.

Ten points ranging from 2100 to 3000 K were obtained in the first set-up (see Fig. 4). We could deduce $\alpha = (3.48 \pm 0.45) \times 10^{-5} \text{ K}^{-1}$. With the second set we obtained 17 points from 2000 to 2900 K and compared these points directly with those of a free cooling sequence recorded from 3100 K with the same optical settings. Some points in the range of 2600 to 3000 K could not be determined because there was not enough contrast between the drop and the nozzle. We observed that the differences between the free cooling and the fixed temperature results is less than 2%, which is satisfactory since it is of the same order as the amplitudes of the fluctuations during free cooling.

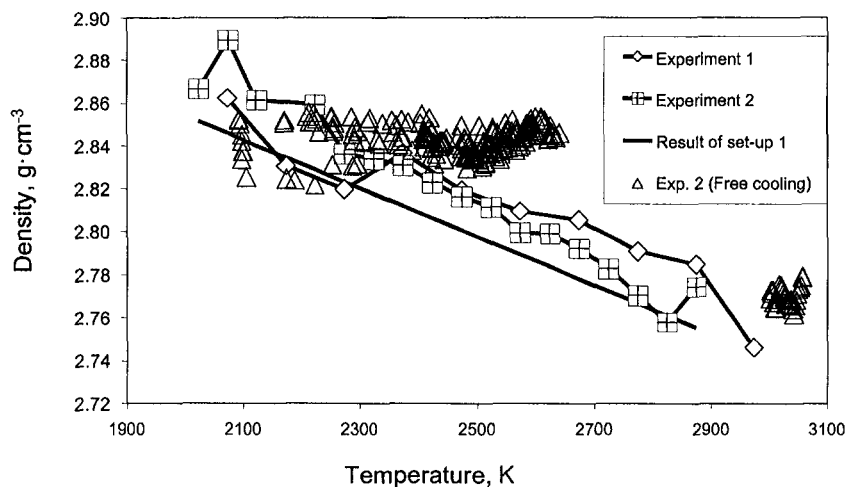


Fig. 4. Estimated density of liquid alumina measured at fixed temperatures.

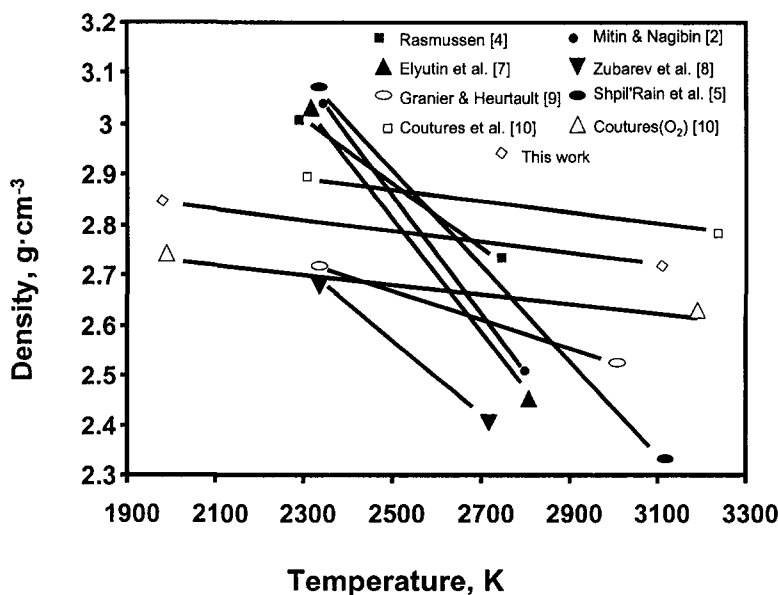


Fig. 5. Density of liquid alumina as a function of temperature.

It is also clear that the scatter of the experimental points obtained with the fixed temperature technique is quite good (less than 1%). From a linear regression of these points, we obtain $\alpha = (4.84 \pm 0.22) \times 10^{-5} \text{ K}^{-1}$.

These experiments demonstrate that there is no significant systematic error introduced by the statistic fluctuations of the density observed during the free cooling of a drop since we obtain α values which are comparable with different techniques.

Our data are compared with literature values in Fig. 5. We observe that all the measurements with contactless methods have similar temperature coefficients, while measurements obtained in crucibles have larger variations. This observation may emphasize the importance of the chemical pollution of measurements with crucibles.

4. CONCLUSION

The combination of aerodynamic levitation, laser heating, a high-speed videocamera, and an image processing system has proved to be a powerful tool to measure the density of liquid oxides with a high precision. The density of liquid alumina was determined between 2000 and 3100 K. Results are in good agreement with published data; the thermal expansion

coefficient is smaller in our levitation experiments than for techniques involving contacts with a crucible.

ACKNOWLEDGMENT

We thank the French agency CNES (Centre National d'Etudes Spatiales) for financial support.

REFERENCES

1. A. D. Kirshenbaum and J. A. Cahill, *J. Inorg. Nucl. Chem.* **14**:283 (1960).
2. B. S. Mitin and Y. A. Nagibin, *Russ. J. Phys. Chem.* **44**:741 (1970).
3. W. D. Kingery, *J. Am. Ceram. Soc.* **42**:6 (1958).
4. J. J. Rasmussen, *J. Am. Ceram. Soc.* **55**:398 (1972).
5. E. E. Shpil'rain, K. A. Yakimovich, and A. F. Tsitsarkin, *High Temp.-High Press* **5**:191 (1973).
6. N. Ikemiya, J. Umemoto, S. Hara, and K. Ogino, *ISIJ Int.* **33**:156 (1992).
7. V. P. Elyutin, B. S. Mitin, and I. S. Annisimov, *Neo. Mater.* **9**:1585 (1973).
8. Y. V. Zubarev, V. I. Kostikov, B. S. Mitin, Y. A. Nagibin, and V. V. Nischeta, *Izv. Akad. Nauk. SSSR Neorg. Mat.* **5**:1563 (1968).
9. B. Granier and S. Heurtault, *Rev. Int. Hautes Temp. Refract.* **20**:31 (1983).
10. J. P. Coutures, J-C. Rifflet, P. Florian, and D. Massiot, *Rev. Int. Hautes Temp. Refract.* **29**:123 (1994).
11. P. Courtial and D. B. Dingwell, *Geochim. Cosmochim. Acta* **59**:3685 (1995).